

Article

Pt Monolayer Electrocatalyst for Oxygen Reduction Reaction on Pd-Cu Alloy: First-Principles Investigation

Amra Peles ^{1,*}, Minhua Shao ² and Lesia Protsailo ³

¹ Physical Sciences Department, United Technologies Research Center, East Hartford, CT 06108, USA

² Department of Chemical and Biomolecular Engineering, Hong Kong University of Science and Technology, Clear Water Bay, Kowloon, Hong Kong; E-Mail: kemshao@ust.hk

³ Pratt & Whitney Program Office, United Technologies Research Center, East Hartford, CT 06108, USA; E-Mail: protsal1@utrc.utc.com

* Author to whom correspondence should be addressed; E-Mail: pelesa@utrc.utc.com

Academic Editor: Keith Hohn

Received: 30 May 2015 / Accepted: 26 June 2015 / Published: 6 July 2015

Abstract: First principles approach is used to examine geometric and electronic structure of the catalyst concept aimed to improve activity and utilization of precious Pt metal for oxygen reduction reaction in fuel cells. The Pt monolayers on Pd skin and Pd_{1-x}Cu_x inner core for various compositions x were examined by building the appropriate models starting from Pd-Cu solid solution. We provided a detailed description of changes in the descriptors of catalytic behavior, d-band energy and binding energies of reaction intermediates, giving an insight into the underlying mechanism of catalytic activity enhancement based on the first principles density functional theory (DFT) calculations. Structural properties of the Pd-Cu bimetallic were determined for bulk and surfaces, including the segregation profile of Cu under different environment on the surface.

Keywords: DFT; core-shell catalyst; electronic structure

1. Introduction

The slow kinetics of the oxygen reduction reaction (ORR) and high cost of platinum electrocatalysts, in the proton exchange membrane fuel cells (PEMFC) are recognized as significant limitations toward the large scale implementation as a clean energy alternative [1–4]. Many research efforts have focused on the search for alternative catalysts with high Pt utilization and improved activity. Pt mono-layer catalyst

supported on metal or metal-alloy core is a promising alternative to the traditional catalysts [5–7]. Enhanced catalytic activity for Pt mono-layer supported on Pd core was demonstrated in Adzic's group [5]. The lateral compressive strain in the Pt surface layer due to the lattice constant mismatch with Pd substrate was suggested as major driving force for the better catalytic activity [8,9]. An alternative view is based on the X-ray photo-electron spectroscopy (XPS) results combined with electrochemical cell. This study concluded that increased coverage of oxygenated reaction intermediates is driving force for enhanced activity for Pt skin like catalyst on bimetallic core [10].

Here we focus on Pt monolayer catalyst deposited on the core that itself has a core-shell structure consisting of Pd shell and $\text{Pd}_{1-x}\text{Cu}_x$ core with $x = 0.125, 0.25, 0.5$ and 0.75 . We provide an insight into the underlying mechanism of catalytic activity enhancement based on the first principles density functional theory (DFT) calculations. In our approach, we examine theoretical descriptors of catalyst behavior: Structural and compositional parameters that correlate with catalytic activity changes including electronic structure effects, described by the mean energy of d-band electrons; the electron occupancy of the d-band and strain effects that modify electronic structure via lateral strain in the catalyst's top layer. We build comprehensive models, bottom-up, with the aim to identify optimal compositions of core-shell structure with promise of better catalytic activity solely based on inherent electronic structure features. In principal, catalyst with exposed base metal Cu is not stable in PEMFC, and Cu is expected to be removed over time due to dissolution in the acidic environment causing the accelerated fuel cell degradation. To ensure stability in acid, PdCu bimetallic must be protected by more stable noble metals. Selective dissolution of Cu in PdCu alloy can lead a core-shell structure where core consists of the PdCu alloy and shell of Pd protective skin [11]. The selective dissolution of alloying components provide for compositional and structural changes that play an important role in manipulating catalytic activity [6,8,9,12,13].

Here, we discuss structural properties and surface segregation profile of Pd-Cu bimetallic; the electronic structure properties and surface reactivity effects of pseudo-morphic Pt and Pd over-layers supported on Pd-Cu alloy. The comparison of the simulation results with experiments will be discussed as well.

2. Computational Method

The first-principles calculations are based on spin-polarized density functional theory (DFT) using a Generalized Gradient Approximation (GGA) [14] and projector augmented wave (PAW) method [15] as implemented in Vienna Ab-Initio Simulation Package (VASP) [16,17]. The cut-off energy for plane wave basis set was 400 eV and Brillouin zone was sampled using a Monkhorst-Pack sampling technique [18] with k-space interval Δk not larger than 0.3 \AA^{-1} . Surfaces are modeled by 8-layer slabs with 2×2 surface cell separated by a 16 \AA vacuum layer perpendicular to the surface. The top six layers were fully relaxed until Hellmann-Feynman forces were 0.01 eV/\AA . The Pt and Pd monolayer surfaces are modeled as pseudo-morphic layers placed on top of the $\text{Pd}_{1-x}\text{Cu}_x$ (111) surface.

3. Results and Discussion

3.1. Structural Properties of $Pd_{1-x}Cu_x$

Pd and Cu, both crystallize in the face centered cubic (fcc) geometry with $Fm\bar{3}m$ space group. Binary phase diagram [19–21] of Pd-Cu bimetallic, shows formation of the solid state solution along the entire range, x , of $Pd_{1-x}Cu_x$ compositions above 600 °C. The ordered phases have been reported at lower temperatures. Here we investigate solid solution phases as our theoretical results were compared to the samples which were synthesized at 700 °C and subsequently subjected to dealloying [11]. Bimetallic solid solution structures were optimized by minimizing forces on atoms for the range of lattice parameters between those of Pd and Cu in $4 \times 4 \times 4$ super-cell geometry for each composition $x = 0, 0.125, 0.25, 0.5, 0.75$ and 1 in $Pd_{1-x}Cu_x$. Super-cell is illustrated in Figure 1a. Two random atomic distributions in solid state solution were considered for each x and final lattice parameter represents an average over the two. Equilibrium lattice parameters were obtained by fitting energy *versus* volume curves, shown in Figure 2, to the third order Birch-Murnaghan equation of state as follows:

$$E = E_0 + \frac{9V_0B_0}{16} \left\{ \left[\left(\frac{V_0}{V} \right)^{\frac{2}{3}} - 1 \right]^3 B'_0 + \left[\left(\frac{V_0}{V} \right)^{\frac{2}{3}} - 1 \right]^2 \left[6 - 4 \left(\frac{V_0}{V} \right)^{\frac{2}{3}} \right] \right\} \quad (1)$$

We also generated and optimized the special quasi random structures [22] at these compositions that have lead to the lattice parameters within 0.1 Å of those found by fitting equations of state. Calculated lattice parameters of Pd and Cu are 3.96 and 3.64 Å, respectively. Figure 1b displays the dependence of lattice parameter of disordered structures to the composition constant x . The computed linear changes follow empirically observed Vegard's law.

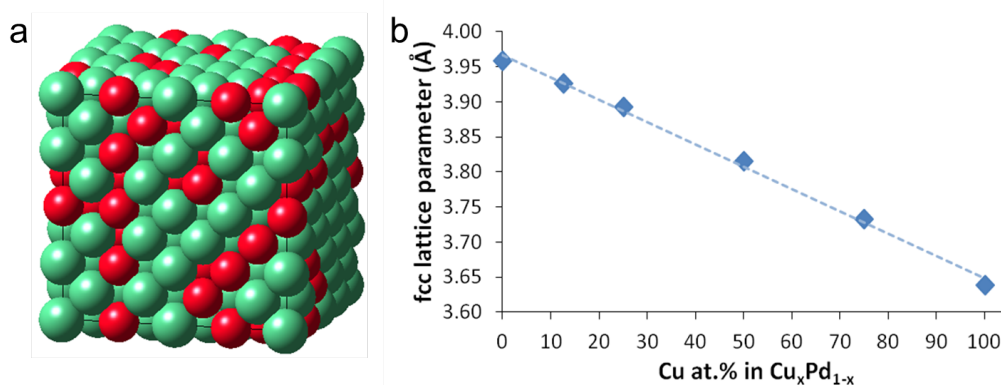


Figure 1. (a) Super-cell illustration. (b) Calculated lattice parameters for solid state solution of $Pd_{1-x}Cu_x$ for various compositions x .

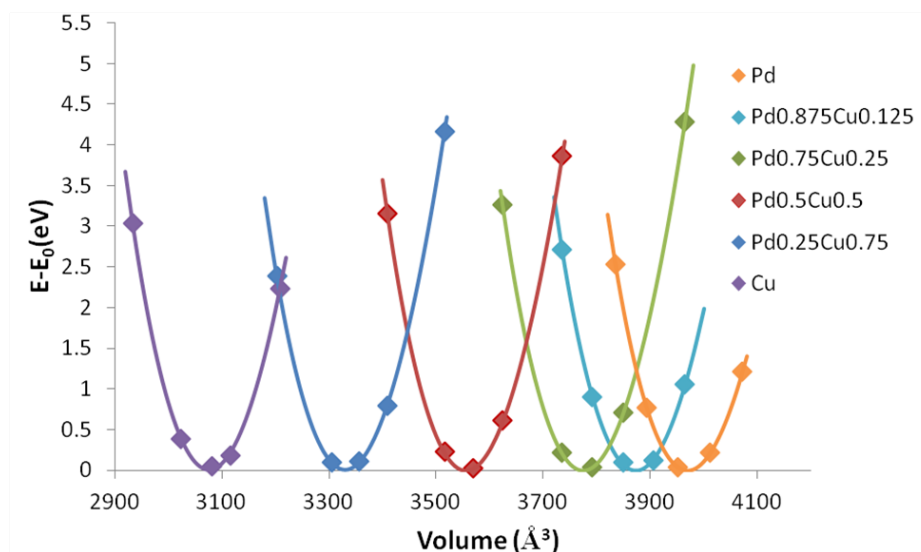


Figure 2. The total energy as a function of the super cell volumes and a Birch-Murnaghan fits to the calculated points for $\text{Pd}_{1-x}\text{Cu}_x$; $x = 0, 0.125, 0.25, 0.5, 0.75$ and 1. The zero of the energy is set to the minimum of each curve, while volumes are given in \AA^3 .

3.2. Chemical Stability and Segregation Profile

Chemical stability of $\text{Pd}_{1-x}\text{Cu}_x$ solid state solutions is examined by calculating formation enthalpy as follows:

$$\Delta H = E_{\text{Pd}_{1-x}\text{Cu}_x} - [(1-x)E_{\text{Pd}_{1-x}} + xE_{\text{Cu}_x}] \quad (2)$$

where $E_{\text{Pd}_{1-x}}$, E_{Cu_x} and $E_{\text{Pd}_{1-x}\text{Cu}_x}$ are the free energies per atom of pure Pd, pure Cu, and the PdCu alloy at concentration x , respectively.

Chemical compositions of alloys at surfaces often differ from the bulk composition and depend on the chemical environment. In bimetallics, surface composition may become enriched by one of the alloying components. To understand which alloying components enriches the surface under the neutral and strongly interacting environment, we have computed Cu segregation energies for the (111) slabs in vacuum and with oxygen adsorbed on the surface. Segregation energy is computed as energy difference for total slab energies with Cu enriched and Pd depleted surface $E_{\text{Cu}\uparrow\text{Pd}\downarrow}$ and stoichiometric surface E_{stoich} according to:

$$E_{\text{seg}}^{\text{Cu}} = E_{\text{Cu}\uparrow\text{Pd}\downarrow} - E_{\text{stoich}} \quad (3)$$

where negative (positive) energy favors (disfavors) surface segregation of copper. Results are summarized in Table 1. Formation enthalpy is negative and increases with increased amount of Pd, with the exception of $x = 0.5$ which presents an ordered alloy. Negative enthalpy indicate chemically stable solid solutions with stability increasing with increased amount of Pd. The trends in copper segregation are different in vacuum and in oxygen. Cu tends to segregate to the surface of solid solutions in strongly reacting oxygen environment while in inert environment, as in vacuum, Pd enriches the surface. This tendency have important consequences for PEMFC application. Exposure to the acidic conditions leads to strong interaction of more abundant copper species on the surface and their

subsequent dissolution. With careful de-alloying strategy, catalyst with surface layer covered by noble Pd metal skin and bimetallic PdCu core can be engineered [11].

Table 1. Formation enthalpy ΔH (meV/atom) and surface segregation energy of Cu E_{seg}^{Cu} (meV).

Composition	ΔH	E_{seg}^{Cu} in vacuum	E_{seg}^{Cu} in oxygen
Pd _{0.875} Cu _{0.125}	−29.68	-	-
Pd _{0.75} Cu _{0.25}	−54.84	61	−100
Pd _{0.5} Cu _{0.5}	−95.47	72	−136
Pd _{0.25} Cu _{0.75}	−79.88	70	−178

3.3. Electronic Structure

Oxygen reduction reaction (ORR) in PEMFC require a catalyst that can speed up interaction of oxygen from the air with recombined electron and proton to form water as a product:



The potency of precious metal catalyst has been correlated with the position of electronic d-band center at catalyst surfaces, since d electrons are involved in making and breaking of inter atomic bonds of ORR reactants and products. We have examined changes in the position of d-band center with respect to Fermi level, associated with Pd atoms on the Pd monolayer surface commensurate with Pd_{1-x}Cu_x substrate and compare them to the pure Pt. Figure 3 illustrate these changes, showing the shift in the positions of d-band center which start decreasing with the amount of copper in the Pd-Cu core and asymptotically approaches position of d-band center of Pt, illustrating a modification of physical properties at atomic scale that make Pd on substrates to behave in between pure Pd and Pt becoming more like Pt metal with increasing amount of Cu in the substrate.

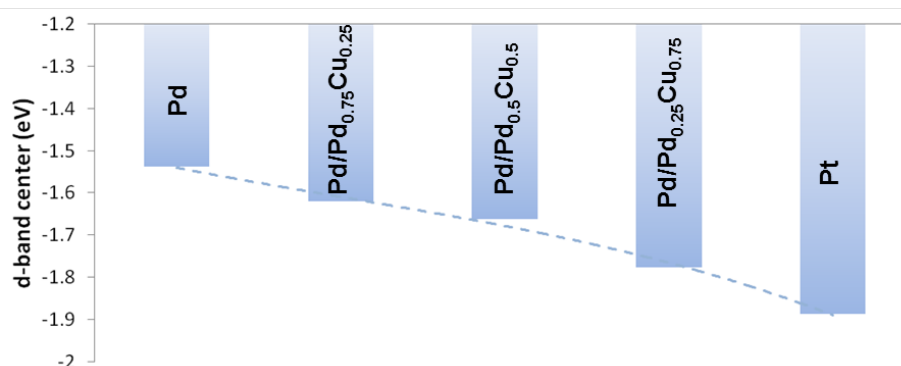


Figure 3. Changes in the position of Pd d-band center with respect to Fermi level on Pd_{1-x}Cu_x substrates.

The changes in the d electrons density of state of surface Pt, modeled as pseudo-morphic layer on Pd/Pd_{1-x}Cu_x are shown in Figure 4. Pt 5d projected electron density of states becomes broader with

increase in Cu content. The marked positions of d-band center shift away from the Fermi level when Cu content increases. The shifts of d-band center value away from the Fermi level indicate a surface of lower adsorption affinity to the ORR intermediates. The ability of surface to interact with adsorbate molecules can be measured by the strength of the adsorbate-surface bond. Binding energies for O and OH reaction intermediates were computed with respect to respective gas phase.

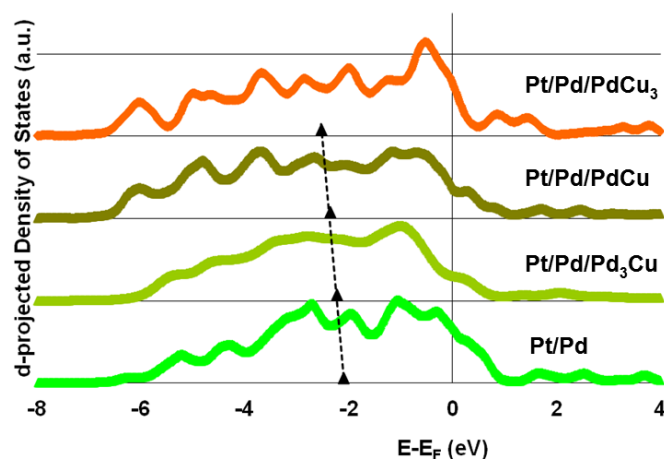


Figure 4. Calculated d-projected density of states of Pt mono-layer for Pd/Pd_{1-x}Cu_x substrates and Pt metal. The Fermi level is set at zero. The position of d-band center, marked by black triangles, shift away from Fermi level for Pt on mixed Pd_{1-x}Cu_x substrates.

$$E_O = E_{slab+O} - E_{slab} - \frac{1}{2}E_{gas}(O_2) \quad (5)$$

$$E_{OH} = E_{slab+OH} - E_{slab} - E_{gas}(OH) \quad (6)$$

The correlation of changes in the position of d-band center and surface reactivity, the strength of adsorbate-surface interaction are presented in Figure 5 for intermediates of ORR reaction. The OH intermediates bind on the top of Pt sites, while atomic oxygen intermediates bind on the hollow sites at (111) and more favorably on sites with fcc symmetry. The bonding strength of ORR intermediates decreases on surfaces with d-band center shifted away from the Fermi level.

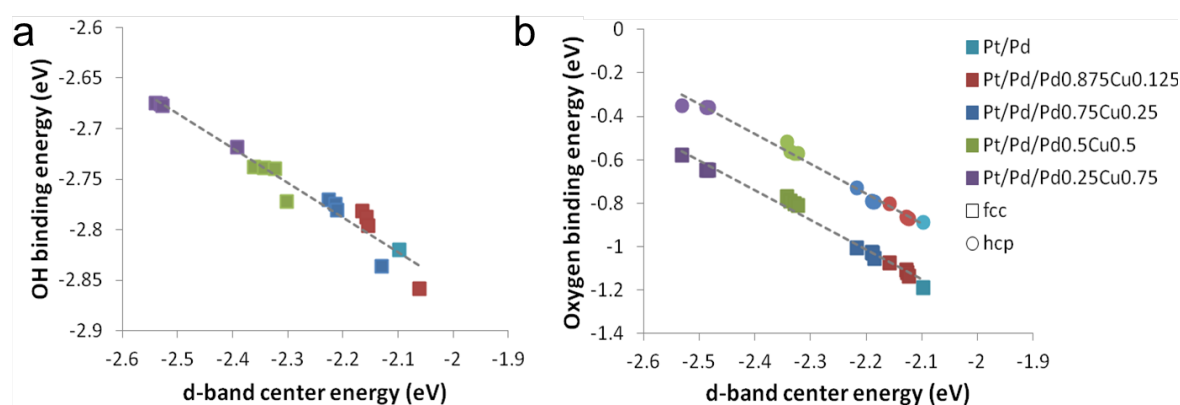


Figure 5. The correlation between surface binding strength and position of the d-band center for oxygen reduction reaction (ORR) intermediates: (a) OH species on the top sites and (b) oxygen atoms on fcc and hcp hollow sites.

The optimal catalytic activity per active site is a trade-off between a not too strong and a not too weak binding of reaction intermediates on the catalyst surface. Empirical observations show the volcano type dependence between catalytic activity and surface reactivity [7,23–25]. The maximum of the volcano plot defines most optimal catalyst. According to this principle, the rate limiting step for ORR on Pt metal is its too strong binding of oxygen in the multi-step ORR reaction. The catalysts that bind oxygen less strongly than Pt but still not too weakly, that this would become rate limiting step, hold the promise of better catalytic activity. The change toward lower binding energy of 0.2 eV have been suggested as optimal in literature [6]. Such shift is accomplished in the case of Pt/Pd/Pd_{1-x}Cu_x; ×0.125; shown in the Figure 5. Indeed the experimental evidence for the activity of Pt mono-layer on the electrochemically de-alloyed Pd-Cu alloy, characterized to have Pd skin on the core corresponding to the Pd_{0.85}Cu_{0.125} resulted in the catalyst with way superior catalytic activity compared to Pt metal [11].

4. Conclusions

We presented the comprehensive build-up of models accounting for various compositions of the Pt and Pd monolayers on Pd_{1-x}Cu_x alloys with $x = 0, 0.125, 0.25, 0.5, 0.75$ and 1. Surface segregation profile shows different segregation tendency and surface compositions for models in vacuum and with adsorbed oxygen, pointing to the limiting stability factors for the PEMFC applications. Detailed study of the d-electrons projected electronic density of states and position of d-band center energy is presented. The correlation between the d-band center energy of surface atoms and surface reactivity is linear indicating less reactive surfaces for d-band center energy further away from the Fermi level. Relying on the empirical observations based on Sabatier principle, Pt/Pd/Pd_{0.875}Cu_{0.125} was identified as the most optimal composition and geometry that correlates with better catalytic activity compared to pure Pt and Pt/Pd core-shell catalyst. These predictions were corroborated by the experimental results [11].

Author Contributions

A. P. conceived and designed computational models, performed the computations, analyzed the data, predicted the optimal catalyst composition and wrote the paper; M. S. and L. P. conceived the concept of Pd-Cu core shell catalyst and provided the data for the experimental validation.

Conflicts of Interest

The authors declare no conflict of interest.

References

1. Gasteiger, H.A.; Kocha, S.S.; Sompalli, B.; Wagner, F.T. Activity benchmarks and requirements for Pt, Pt-alloy, and non-Pt oxygen reduction catalysts for PEMFCs. *Appl. Catal. B* **2005**, *56*, 9.
2. Adzic, R.R. Frontiers in electrochemistry. In *Electrocatalysis*; Lipkowsky, J., Ross, P.N., Eds.; Wiley: New York, NY, USA, 1998; p. 197.
3. Gasteiger, H.A.; Markovic, N.M. Just a dream-or future reality? *Science* **2009**, *324*, 48–49.
4. Bashyam, R.; Zelenay, P. A class of non-precious metal composite catalysts for fuel cells. *Nature* **2006**, *443*, 63–66.
5. Adzic, R.R.; Zhang, J.; Sasaki, K.; Vukmirovic, M.B.; Shao, M.; Wang J.X.; Nilekar, A.U.; Mavrikakis, M.; Valerio, J.A.; Uribe, F. Platinum monolayer fuel cell electrocatalysts. *Top. Catal.* **2007**, *46*, 249–262.
6. Stamenkovic, V.R.; Mun, B.S.; Arenz, M.; Mayrhofer, K.J.J.; Lucas, C.A.; Wang, G.; Ross, P.N.; Markovic, N.M. Trends in electrocatalysis on extended and nanoscale Pt-bimetallic alloy surfaces *Nat. Mater.* **2007**, *6*, 241–247.
7. Stamenkovic, V.R.; Fowler, B.; Mun, B.S.; Wang, G.; Ross, P.N.; Lucas, C.A.; Markovic, N.M. Improved oxygen reduction activity on Pt₃Ni (111) via increased surface site availability. *Science* **2007**, *315*, 493–497.
8. Hammer, B.; Nørskov, J.K. Electronic factors determining the reactivity of metal surfaces. *Surf. Sci.* **1995**, *343*, 211.
9. Greeley, J.; Mavrikakis, M. Alloy catalysts designed from first principles. *Nat. Mater.* **2004**, *3*, 810–815.
10. Watanabe, M.; Wakisaka, M.; Yano, H.; Uchida, H. Analyses of oxygen reduction reaction at Pt-based electrocatalysts. *ECS Trans.* **2008**, *16*, 199.
11. Shao, M.; Shoemaker, K.; Peles, A.; Kaneko, K.; Protsailo, L. Pt monolayer on porous Pd-Cu alloys as oxygen reduction electrocatalysts. *J. Am. Chem. Soc.* **2010**, *132*, 9253–9255.
12. Koh, S.; Strasser, P. Electrocatalysis on bimetallic surfaces: Modifying catalytic reactivity for oxygen reduction by voltammetric surface dealloying. *J. Am. Chem. Soc.* **2007**, *129*, 12624–12625.
13. Zeis, R.; Mathur, A.; Fritz, G.; Lee, J.; Erlebacher, J. Platinum-plated nanoporous gold: An efficient, low Pt loading electrocatalyst for PEM fuel cells. *J. Power Sour.* **2007**, *165*, 65.
14. Pedrew, J.P.; Wang, Y. Accurate and simple analytic representation of the electron-gas correlation energy. *Phys. Rev. B* **1992**, *45*, 13244.

15. Blöchl, P.E. Projector augmented-wave method. *Phys. Rev. B* **1994**, *50*, 17953–17979.
16. Kresse, G.; Furthmüller, J. Efficient iterative schemes for ab initio total-energy calculations using a plane-wave basis set. *Phys. Rev. B* **1996**, *54*, 11169.
17. Kresse, G.; Joubert, D. From ultrasoft pseudopotentials to the projector augmented-wave method. *Phys. Rev. B* **1999**, *59*, 1758.
18. Monkhorst, H.J.; Pack, J.D. Special points for Brillouin-zone integrations. *Phys. Rev. B* **1976**, *13*, 5188.
19. Subramanian, P.R.; Laughlin D.E. *Cu-Pd (Copper-Palladium), Binary Alloy Phase Diagrams*, 2nd ed., Massalski, T.B., Ed.; Springer-Verlag: Berlin, Germany, 1990; Volume 2, pp. 1454–1456.
20. Straumanis, M.E.; Yu, L.S. Lattice parameters, densities, expansion coefficients and perfection of structure of Cu and of Cu-In (α) phase. *Acta Crystallogr.* **1969**, *25*, 676.;
21. Rao, C.N.; Rao, K.K. Effect of temperature on the lattice parameters of some silver-palladium alloys. *Can. J. Phys.* **1964**, *42*, 1336–1342.
22. Alex Zunger, A.; Wei, S.H.; Ferreira, L.G.; Bernard, J.E. Special quasirandom structures. *Phys. Rev. Lett.* **1995**, *65*, 353–356.
23. Stamenkovic, V.; Moon, B.S.; Mayrhofer, K.J.J.; Ross, P.N.; Markovic, N.M.; Rossmeisl, J.; Greeley, J.; Nørskov, J.K. Changing the activity of electrocatalysts for oxygen reduction by tuning the surface electronic structure. *Angew. Chem.* **2006**, *45*, 2897–2901.
24. Zhang, J.L.; Vukmirovic, M.B.; Xu, Y.; Mavrikakis, M.; Adzic, R.R. Controlling the catalytic activity of platinum-monolayer electrocatalysts for oxygen reduction with different substrates. *Angew. Chem.* **2005**, *44*, 2132–2125.
25. Greeley, J.; Stephens, I.E.L.; Bondarenko, A.S.; Johansson, T.P.; Hansen, H.A.; Jaramillo, T.F.; Rossmeisl, J.; Chorkendorff, I.; Nørskov, J.K. Alloys of platinum and early transition metals as oxygen reduction electrocatalysts. *Nat. Chem.* **2009**, *1*, 552–556.

© 2015 by the authors; licensee MDPI, Basel, Switzerland. This article is an open access article distributed under the terms and conditions of the Creative Commons Attribution license (<http://creativecommons.org/licenses/by/4.0/>).